ORIGINAL PAPER

Utilization of chemically modified coal fly ash as cost-effective adsorbent for removal of hazardous organic wastes

A. Eteba[1] · M. Bassyouni[2,3] · M. Saleh[4]

Abstract

Disposal of dyes wastewater into aquatic streams is considered as a major challenge due to its effect on water ecosystem. Direct dyes have a complex aromatic structure. Therefore, it is difficult to separate them from industrial wastewater. Conversely, fly ash is a main by-product pollutant generated from coal burning to fulfill energy requirements. In this study, thermochemical treatment process was applied to coal fly ash (CFA) in order to increase its surface area, improve its pore's structure and enhancing its adsorption capacity for direct blue 78 dye (DB78) removal. The treated coal fly ash (TCFA) was characterized by physicochemical analyses such as XRD, XRF, TGA, SEM, FTIR, surface area (S_{BET}) and particles size analysis. Batch experiments were conducted to analyze the adsorption behavior for TCFA and to examine the DB78 dye removal efficiency. The physicochemical analysis results indicated that a higher increase in CFA surface area from 9.6 to 60.4 m^2g^{-1} was obtained due to the modification process. The maximum removal efficiency using TCFA was 99.7% for initial dye concentration 10 mg/L and TCFA dose 2 g/L. The adsorption isotherm was studied by Langmuir and Freundlich model using different dye concentrations. The results showed that equilibrium data followed closely Langmuir isotherm model ($R^2 = 0.99$) indicating monolayer and homogeneous adsorption process.

Introduction

Overgrowing of textile industries has resulted in engender of enormous quantity of liquid wastes which includes organic and inorganic complexes (Qi et al. 2017). It was valued that $\sim 7 \times 10^5$ tons of dyes is produced worldwide per year (Anastopoulos et al. 2017). Some of these produced dyes are

applied in fabrics dying process. During this process, some of these dyes are released from fabrics into water. Major quantity of released dyes is washed out. These released dyes reach 20–30% out of the total direct dye's quantity (Scalbi et al. 2005). Therefore, the effluents wastewater stream from textile industry contains high concentration of complex dyes. Higher organic carbon values than standard limits are found if proper treatment methods were not carried out. Disposal of these dyes wastewater into water reservoirs would lead to color dispersion which stops sunlight transmission into water, thus decreases the photosynthesis and damages the water ecosystem (Wang et al. 2018).

Synthetic dyes are considered as a highly toxic and cancerogenic contaminates because they have a complex aromatic structure leading to difficult decomposition and separation (Mushtaq et al. 2020). There are many types of dyes that's used in fabrics dyeing processes, these types can be categorized into anionic, cationic and non-anionic dyes. Among these, anionic dyes are considered a very toxic type because they are not able to degrade easily or can leach into food chain (Golbad et al. 2017). This may represent a main threat to the environmental ecology and public health if left

✉ M. Bassyouni
m.bassyouni@eng.psu.edu.eg

[1] Sanitary and Environmental Engineering, Department of Civil Engineering, Faculty of Engineering, Port Said University, Port Said, Egypt

[2] Department of Chemical Engineering, Faculty of Engineering, Port Said Unversity, Port Said, Egypt

[3] Center of Excellence in Membrane-Based Water Desalination Technology for Testing and Characterization (CEMTC), Port Said University, Port Said 42526, Egypt

[4] Sanitary and Environmental Engineering, Department of Civil Engineering, Faculty of Engineering, Port Said University, Port Said, Egypt

without proper separation process (Siyal et al. 2020; Rubab et al. 2021; Elhenawy et al. 2020; Abdel-Aziz et al. 2020; Bassyouni et al. 2020; Da Costa Rocha et al. 2020; Sun et al. 2013).

Therefore, with many degrees of success, various forms of dyes removal processes have been studied and applied such as physical, chemical and biological methods (Zarrini et al. 2017). These methods include different criteria and processes such as precipitation–coagulations, aerobic and anaerobic treatment, advanced oxidation, ion exchange, membrane filtration and adsorption (Hussain et al. 2022). However, these treatment technologies showed a number of limitations and disadvantages, including a lower validation in removal of different pollutants, high costs, high reagent requirement and generation of toxic waste products which require further safe disposal.

Among various color removal processes, adsorption is considered as the most versatile treatment technology (Hussain et al. 2022; Gutub et al. 2013; Eteba et al. 2021; Bonilla-Petriciolet et al. 2017; Gong et al. 2008; Al-Ghouti et al. 2003). This technique should be simple, environmentally friendly and able to extract several types of dyes wastes efficiently and low operating cost (Astuti et al. 2019).

Activated carbon was studied as a relatively safe adsorbent because of its ability to remove numerous types of hazardous pollutants from water and wastewater effluent (Bansal et al. 2005). However, it is not frequently used because of its high cost. As a result, significant efforts have been made to develop both conventional and non-conventional inexpensive adsorbents using a variety of materials including coal fly, sawdust, municipal solid waste, red mud, zeolites and sugar industry waste (Crini et al. 2019; Mor et al. 2018; Crini et al. 2006; Ferreroet al. 2015).

Coal is considered as a main natural source of energy which is widely used for many decades. It achieves about 25% of the energy requirements around the world. It was reported that 750 million tons of coal fly ash (CFA) are generated annually, with at least 75% not being managed in an environmentally friendly way. CFA is widely used in many applications such as cement industries, road construction, adsorption and preparation of mesoporous silica and zeolite (Hussain et al. 2022). Coal fly ash is considered an attractive low-cost adsorbent among several industrial solid wastes (by-product) because of its ability to adsorb many types of poisonous and non-biodegradable dyes from colored effluents (Blissett et al. 2012; Dizge et al. 2008; Sarkar et al. 2022).

Raw coal fly ash (CAF) is known by its low surface area, small pores volume and its crystalline structure. Therefore, many modification processes have been applied to CFA using physical and/or chemical methods in order to improve its adsorption capacity for dyes removal (Gao et al. 2015; Banerjee et al. 2014). It was reported that, the chemical treatment of CFA using HCl increased its surface area from 4.5 to 13.49 m^2g^{-1} (Hussain et al. 2022). Increase surface area of raw fly ash and its adsorption capacity for anionic dyes removal are still insufficiently explored. To fill this literature gap, this paper studied the effective chemical treatment method to achieve remarkable increase in the surface area of treated fly ash with high removal efficiency of anionic dyes. The surface area of treated CAF was increased from 9.6 to 60.4 m^2g^{-1} and improved its removal efficiency up to 99%. The results showed that the mesoporous TCFA was successfully synthesized in this study.

Materials and methods

Adsorbent materials and dyes

The raw coal fly ash (RCFA) samples were obtained from a cement factory result from burning of pulverized coal. These samples were sieved and particles that have size less than 75 μm (pass from sieve no-200) were used in this study. RCFA samples were washed using a distilled water, filtered and left to dry at 110 °C for 12 h. In order to obtain treated coal fly ash (TCFA), RCFA samples were modified using HCl solution (30% w/w) at 90 °C for 12 h. At the end of modification process, the mixture was filtrated, washed using a distilled water and left to dry at 120 °C for 24 h. Finally, TCFA was characterized using physical and chemical analysis.

The direct blue 78 (DB78) dye with commercial name (Tubantin GLL 300), relative molecular weight 1059.95 g/mol, max wave length $\lambda_{max} = 604$ nm and solubility up to 10 g/L at 25 °C was selected for adsorption process. The chemical structure of DB78 dye is illustrated in Fig. 1.

Fig. 1 Chemical structure of direct blue 78 dye (Tubantin blue GLL 300)
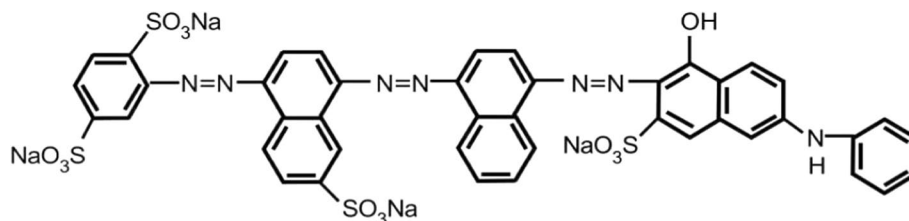
Three synthetic dye solutions with different dye concentrations (10, 20 and 30 mg/L) were prepared for adsorption study.

It was reported that DB78 dye has a high harmful effect on environment because it has a high-water solubility, making it extremely difficult to be extracted using traditional methods. One of its characteristics is the capacity to spread color to a given substrate due to its molecular structure which contains chromophoric groups. These colors disrupt the water bodies aesthetically, contributing to a decline in the rate of photosynthesis and dissolved oxygen levels affecting the entire aquatic biota (Lellis et al. 2019).

Characterization of adsorbent

The phases of RCFA and TCFA samples were examined by XRD analysis with Empyrean diffractometer system using an anode material Cu and operated at 45 kV and 30 mA over the range 5–90° with step size (2Th.) of 0.026, scan step time 21.42 s and Goniometer radius 240 mm. These measurements were conducted at 25 °C.

The chemical composition (XRF analysis) of TCFA samples was conducted using (Axios Advanced, Sequential WD_XRF Spectrometer, analytical 2005, Malvern, UK).

The surface area of RCFA and TCFA samples was determined using N_2 adsorption under (−195.65 °C) using surface area analyzers (ASAP 2020 V4.02) and (St 4 on NOVA touch 4LX). Prior to adsorption studies, the samples were degasified at 200 °C for 4 h. By applying BET (Brunauer–Emmett–Teller) equation to adsorption data, the BET surface area for the samples was measured.

The surface morphology and porous microstructure of RCFA, TCFA and exhausted fly ash (after adsorption process) samples were investigated by SEM analysis using (Quanta 250 FEG scanning electron microscope).

The thermal stability of TCFA and exhausted CFA samples were investigated using thermogravimetric analyzer (LABSYS evo—Setaram).

The FTIR studies for TCFA and exhausted CFA samples were studied using VERTEX 80v vacuum FTIR spectrometer.

The particles size analysis was conducted using Particle Sizing Systems\ZPW388- V2.14\zpw388.tbl. The wavelength used was 632.8 nm and sample temperature of 23 °C.

The colorimetric analysis was performed in this study using LAMOTTE smart spectrophotometer v3 2000-01-MN, USA.

The pH of RCFA and TCFA samples was determined by mixing of 0.1 g from sample with 100 mL of distilled water, mixing speed was 100 r.p.m, for 3 h at 25 °C using digital pH meter, omega CDS107, Taiwan.

Adsorption studies

This study was conducted by discontinuous batch adsorption system on a single component synthetic wastewater. TCFA was prepared to enhance the adsorption capacity with applied doses range (0.5–5) g in 1000 mL of synthetic dye solutions, contact time rang (0–30) min, mixing speed 500 r.p.m and temperature (25 ± 2 °C). The adsorption experiments were conducted with different initial concentrations (10, 20 and 30) mg/L. The spectrophotometrically method was applied in order to determine the removal efficiency by measuring dyes concentration before and after adsorption process at $\lambda_{max} = 600$ nm for DB78 dye.

Results and discussion

Characterization of adsorbent

Because of the importance and great influence of particles size on adsorption process, raw coal fly ash was measured and is demonstrated (Gaussian distribution analysis) in Fig. 2. It was observed that 99% of the RCFA particles have a size less than 5.7 μm. As has been previously reported in the literature that there is an inverse relationship between particles size and adsorption capacity. The smaller the fly ash particles size, the higher the available surface area which leads to a maximum adsorption capacity (Blissett et al. 2012).

Figure 3 shows the X-ray diffraction of RCFA with a particle size ≤ 75 μm. It was found that the RCFA sample consists of some crystalline sharp peaks resulting from the presence of some minerals phases (specific chemistry) such as quartz, mullite, hematite and lime (calcium oxide) and some amorphous phases caused by the presence of a chemically stable glassy surface layer forming by quartz which characterized by a very strong intensity and mullite. Due to this glassy surface layer, the RCFA is less active and chemically stable since it covers the fly ash inner constituents which have a porous, brittle and spongy particles.

In order to disintegrate the chemical stability of the raw coal ash and stimulate the chemical activity, this glassy surface layer (amorphous phase) should be destroyed by a chemical reaction. Thus a chemically modified coal fly ash was applied. Chemical reaction between raw fly ash and hydrochloric acid (HCl) was conducted. As a result of that reaction, the glassy surface layer covering inner particles of the fly ash was eroded. The outer layer was exposed to the acid solution leading to chemical reaction that fractured the coal fly ash particles. Consequently, the sharp crystalline peaks intensity was decreased (some phases were destroyed) and amorphous phases were reduced compared with raw fly ash XRD analysis as shown in Fig. 4. This chemical
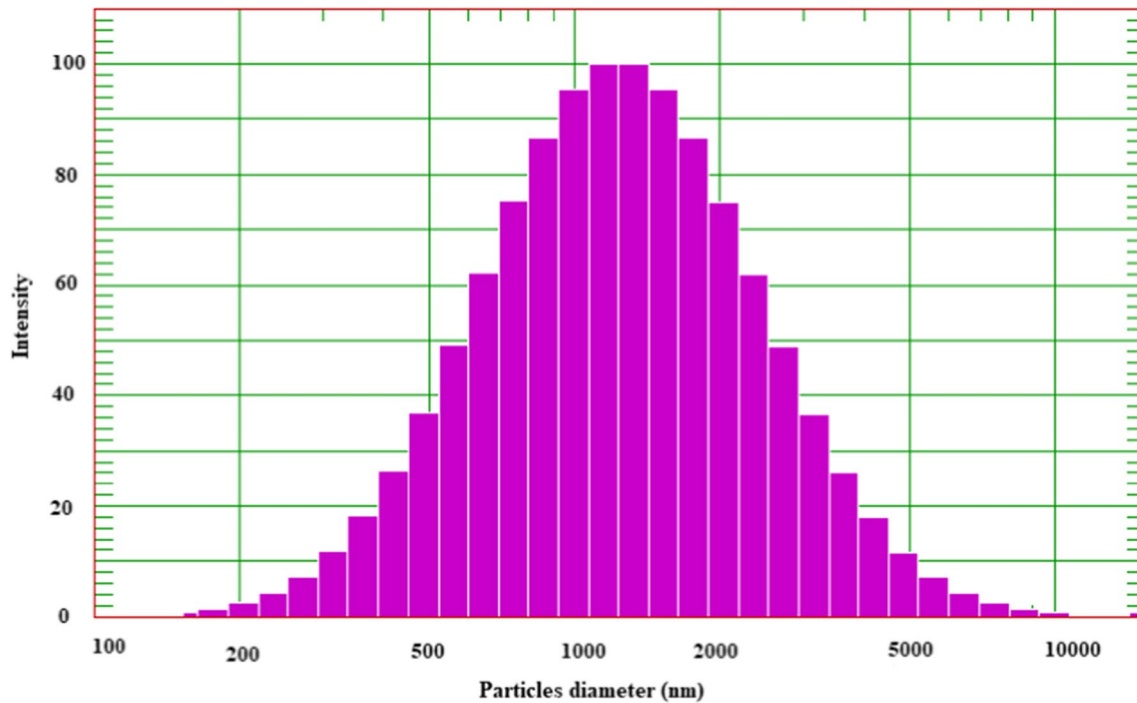
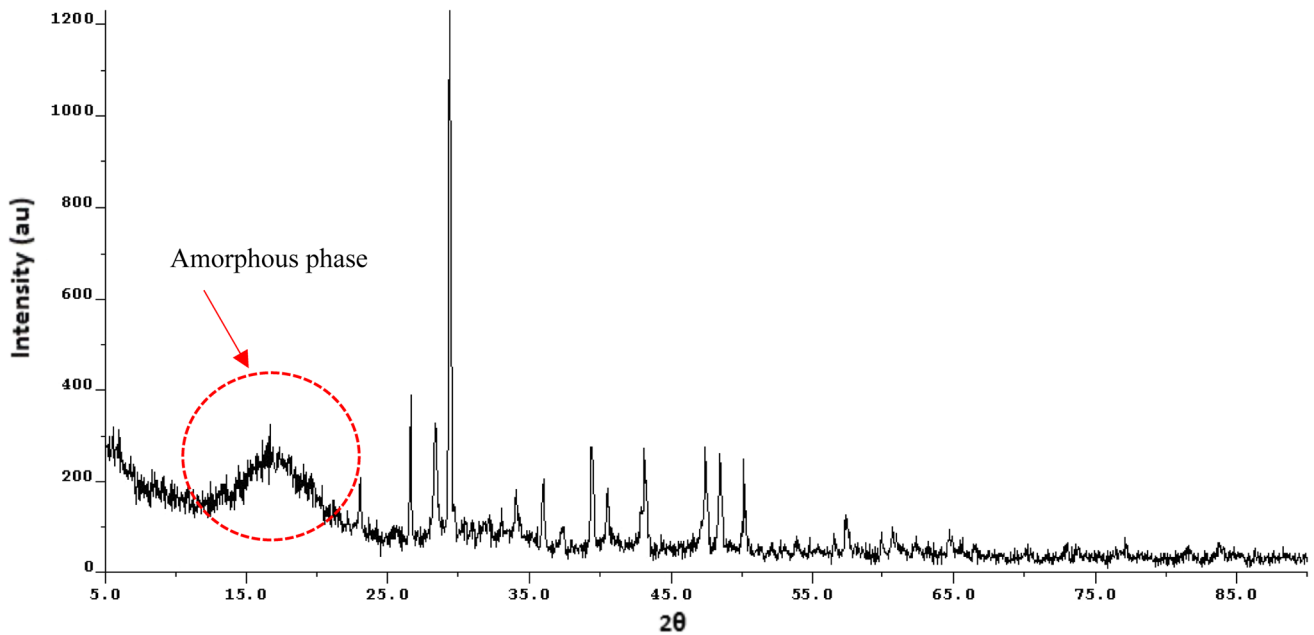**Fig. 2** Intensity-weighted Gaussian distribution analysis for RCFA sample

Fig. 3 X-ray diffraction pattern for the RCFA

treatment led to increase porous volume and surface area which positively affect the adsorption process (Bada et al. 2008).

X-ray fluorescence (XRF) analysis showed that chemical compositions of TCFA are 35.47% lime (CaO), 3.16% silica (SiO_2), 0.66% alumina (Al_2O_3), 0.07% titanium dioxide (TiO_2), 2.57% magnesium oxide (MgO), 0.93% hematite (Fe_2O_3), 0.80% sodium oxide (Na_2O), 1.20% potassium oxide (K_2O), 4.86% phosphorus pentoxide (P_2O_5), 2.21% sulfur trioxide (SO_3), 6.18% chlorine (Cl) and LOI (41.56%).

Trace elements including MnO, NiO, CuO, ZnO, PbO and SrO were found in the TCFA sample. The XRF (elemental analysis) was found in a good agreement with XRD results particularly with the presence of silicon compound (quartz), aluminum compound (mullite) and calcium oxide (lime). Table 1 states the results of XRF analysis for TCFA.

The high value of unburnt carbon observed from XRF analysis (41.56%) was reflected on thermogravimetric analysis for RCFA, TCFA and exhausted TCFA as shown in Fig. 5.

In order to investigate the thermal stability of RCFA, TCFA and exhausted TCFA samples, a small amount of the samples were heated up to 1000 °C with rate 10 degree/min in a temperature-stable and inert crucible made of platinum in a furnace. During the analysis, the samples chamber was flushed with pure nitrogen gas to avoid oxidation.
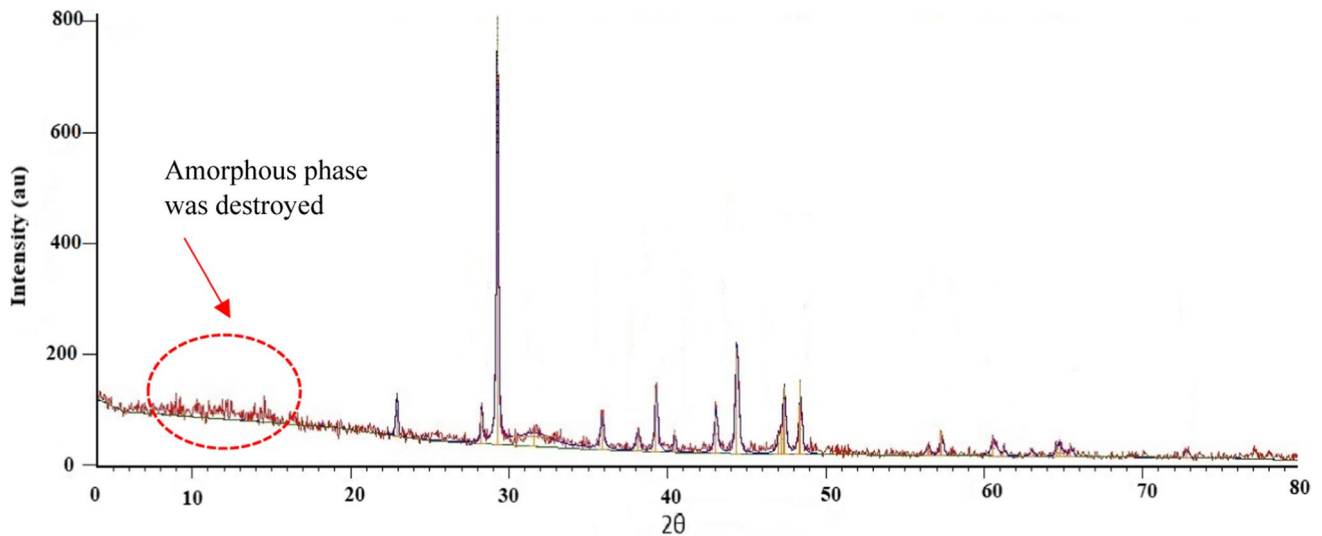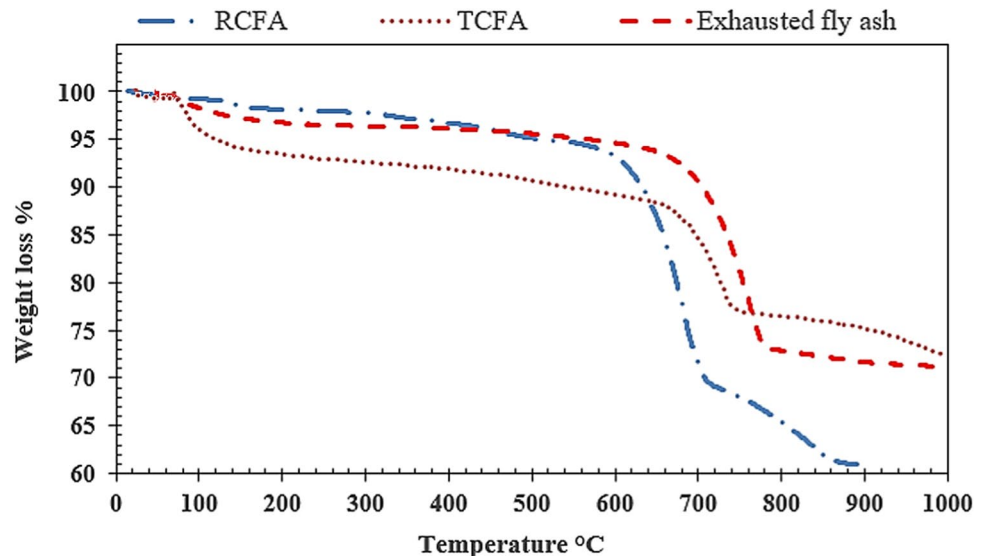

Fig. 4 X-ray diffraction pattern for TCFA

Table 1 XRF analysis results for treated coal fly ash sample

Constituents	SiO_2	Al_2O_3	CaO	P_2O_5	SO_3	Cl	K_2O	MgO	Fe_2O_3	Na_2O	LOI
Weight %	3.16	0.66	35.47	4.68	2.21	6.18	1.2	2.57	0.93	0.80	41.56

Fig. 5 Thermogravimetric analysis curve (TGA) for RCFA

Thermogravimetric analysis (TGA) showed that the chemically treatment of coal fly ash with HCl has a significant effect on its thermal stability. The chemical reaction between fly ash constituents and hydrochloric acid causes demolition and removal of amorphous elements. Therefore, the resulting ash is more efficient in terms of thermal stability. The second stage of thermal decomposition of raw coal fly ash was observed at ~600 °C. After chemical treatment, the second stage started at ~700 °C. In the case of exhausted fly ash, the thermal degradation of adsorbate (direct blue 78 dye) was started after water evaporation at 120 °C due to the decomposition of organic matters.

The BET surface area is about 9.61 m^2g^{-1} and 60.42 m^2g^{-1} for raw coal fly ash and chemically treated coal fly ash, respectively, as listed in Table 2. The remarkable increases in the surface area can be attributed to the chemical reaction between fly ash constituents and HCl which erodes the outer surface of fly ash particles in solution. The chemical reaction not only demolished the morphology of the fly ash surface but also created a large porous structure.

The surface morphology of raw fly ash treated fly ash and exhausted fly ash was studied using SEM analysis in order to examine the impact of the chemical treatment using hydrochloric acid on fly ash particles surface. The raw fly ash particles (as received) have a slick surface with a limit porous structure as observed in SEM image (Fig. 6a). After the chemical modification process, the fly ash particles surface has a noticeable variation. The surface converted from slick surface to porous surface (rough surface) with large improvement of porous structure as observed in SEM image (Fig. 6b). The SEM analysis results are in a good agreement with BET surface area measurements for raw and modified fly ash. After adsorption, the exhausted fly ash was completely loaded and all porous structure and outer surface were blocked with dyes molecules. This can be observed in SEM image (Fig. 6c).

In order to identify the main infrared (IR) bands of organic, minerals and the adsorption mechanism (physical adsorption or chemical adsorption), the treated coal fly ash (before adsorption process) and exhausted treated coal fly

Table 2 Physicochemical properties of raw fly ash and chemically treated fly ash

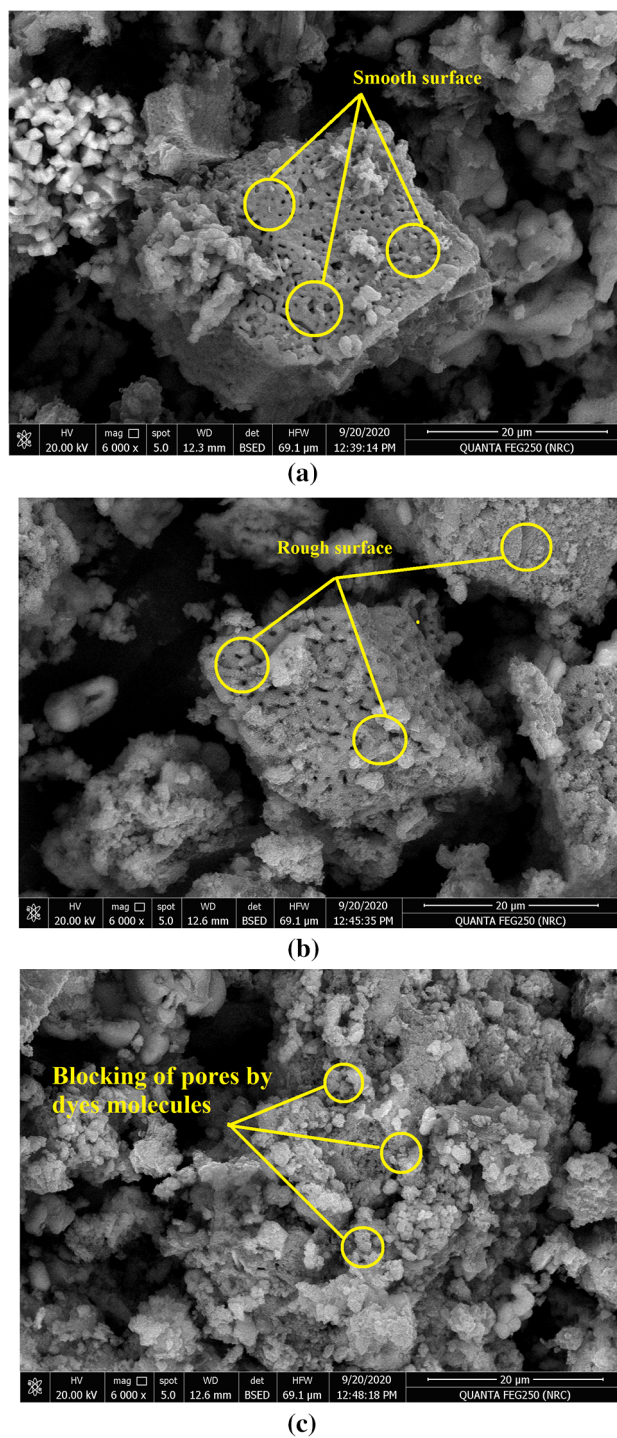| Parameter	Value
BET surface area SBET (RCFA)	9.6113 m^2g^{-1}
BET surface area SBET (TCFA)	60.4199 m^2g^{-1}
Maximum pore volume (RCFA)	0.0149 cm^3g^{-1}
Average particles size (RCFA)	624.26 nm
Median pore width (RCFA)	25.636 nm
pH for raw coal fly ash	11.50
pH for treated coal fly ash	9.70

Fig. 6 SEM images for **a** raw fly ash, **b** modified fly ash and **c** exhausted fly ash

ash (after adsorption process) samples were investigated using FTIR analysis as shown in Fig. 7. The band range of functional group is listed in Table 3. Figure 7 shows that there are nine main peaks having a higher transmittance (%) at different wave numbers (cm^{-1}).

Fig. 7 FTIR spectra for TCFA before and after adsorption process
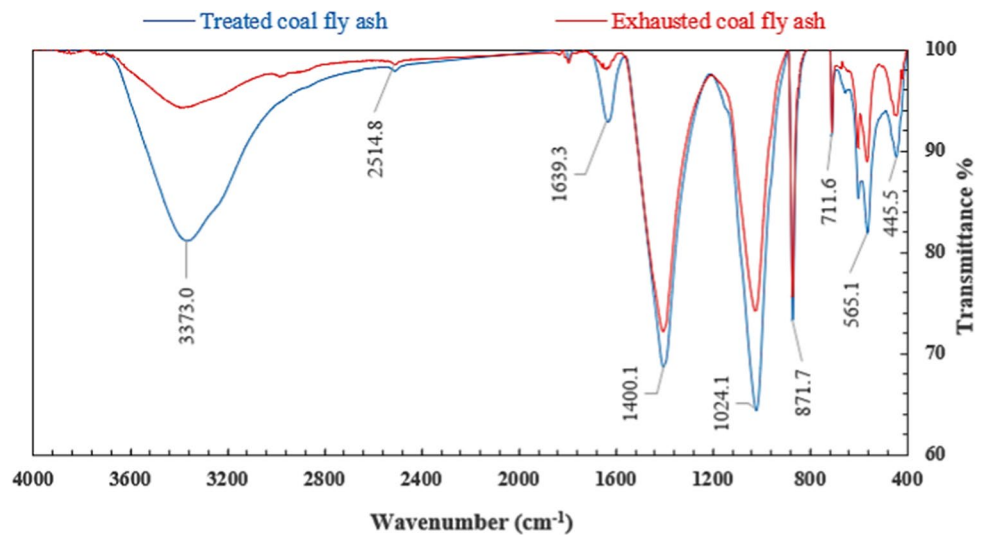
Table 3 Results of FTIR analysis for fly ash before and after adsorption process

Wave number (cm^{-1}) Treated fly ash	Wave number (cm^{-1}) Exhausted fly ash	Band range (cm^{-1})	Indication	References
445.8	451.8	< 500	Bending vibrations of Si–O–Si and O–Si–O bonds	(Fauzi et al. 2016)
564.5	566.6	500–800	Symmetric stretching of Si–O–Si and Al–O–Si	(Fauzi et al. 2016)
602.9	604.1			
711.3	711.6			
871	872	800–1000	Loss of gel CaCO$_3$	(Fauzi et al. 2016)
1022	1025.7	1000–1600	Gains Si–O–Si bands typical of quartz	(Fauzi et al. 2016)
1405.5	1407			
1633.8	1641.4	–	Organic matter (C=O carboxylate group of organic matter)	(Jeyageetha et al. 2016)
–	1796	1600–3500	Stretching (–OH), bending (H–O–H)	(Jeyageetha et al. 2016)
3370.2	3397.32			

The first peak with wave number 445.80 cm^{-1} (less than 500 cm^{-1}) indicates the bending of the Si–O–Si and O–Si–O bonds. For second, third and fourth peaks with wave number 564, 602 and 711 cm^{-1}, respectively (band area detail of 500–800 cm^{-1}) indicates the symmetric stretching of the Si–O–Si and Al–O–Si bands. For fifth peak with wave number 871. cm^{-1} (band area detail of 800–1000 cm^{-1}) indicates the loss of CaCO$_3$. The sixth and seventh peaks with wave number 1024 and 1400 cm^{-1} (band area detail of 1000–1600 cm^{-1}) indicate the gains of Si–O–Si bond typical of quartz. For eighth peak with wave number 1633 cm^{-1} indicates organic matter (C=O carboxylate group of organic matter) (Jeyageetha et al. 2016). The last peak with wave number 3370 cm^{-1} (band area detail of 2800–3400 cm^{-1}) indicates the strongly hydrogen bond Si OH group and adsorbed molecules of water H–O–H bonds (Fauzi et al. 2016).

The FTIR spectra for exhausted treated coal fly ash (after adsorption process) are shown in Fig. 7. It was observed that no discernible difference was found when compared with treated coal fly ash before adsorption process. Only one peak appeared with wave number 1796 cm^{-1} (band area detail of 1600–3500 cm^{-1}) indicating stretching (–OH) and bending (H–O–H). All other peaks have similar wavelength. It was concluded from these results that no difference in the chemical bands from FTIR analysis for fly ash before and after adsorption process that's means the adsorption mechanism is physisorption.

Fig. 8 (**a**) Effect of amount of adsorbent (TCFA) on dye elimination (temperature 20 °C, pH 8.60, mixing speed 500 r.p.m, contact time 30 min and particles size < 75 μm). **b** Effect of amount of adsorbent (TCFA) on adsorbent loading (temperature 20 °C, pH 8.6, mixing speed 500 r.p.m, contact time 30 min and particles size < 75 μm)
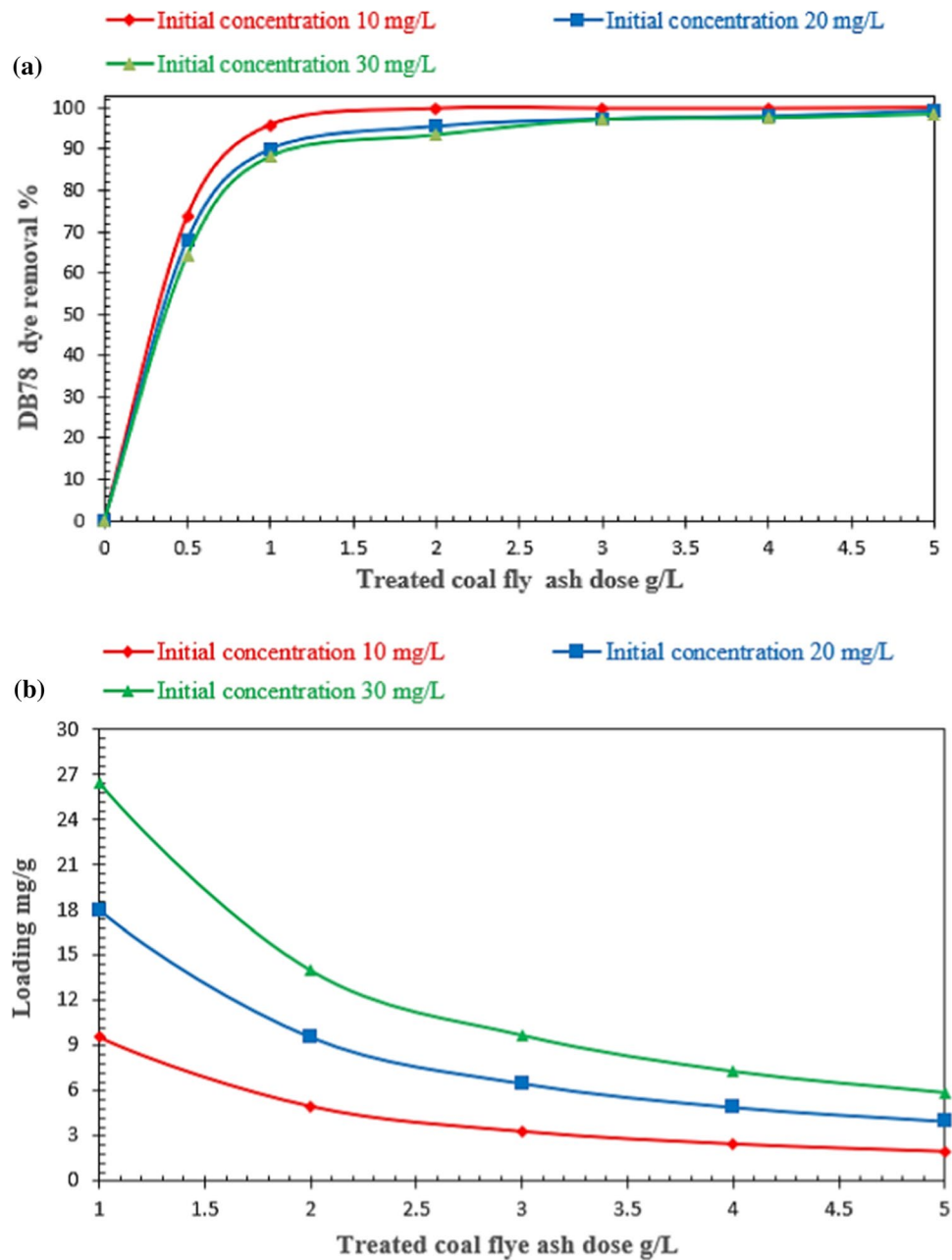
Adsorption tests

Effect of adsorbent dose on dyes removal

Figure 8a shows that the removal of dye from solution increases with increasing of adsorbent dose until reaching the maximum removal percentage and then approximately reaching a constant value. Dyes removal % was studied using different loadings of treated coal fly ash from 0.5 to 5 g/L. Adsorption of synthetic dye was investigated with different initial concentrations (10, 20 and 30) mg/L at constant pH, temperature, mixing speed and contact time.

The results showed that the maximum dyes removal percentage reached 99.7% by using 4 g/L of TCFA at initial dye concentrations (10, 20 and 30) mg/L. Notably, equilibrium loading decreases as TCFA loading increases. The equilibrium loading showed no influence at high TCAF dose > 4 g/L as shown in Fig. 8b. This can be attributed to the large number of potential adsorption sites on TCFA.

The chemical modification process showed a remarkable improvement in adsorption capacity of TCFA as listed in Table 4. For synthetic solution with initial dye concentration 10 mg/L, the removal efficiency is 99.7% using 2 g/L of TCFA. At higher concentration of initial concentration, removal efficiency reached 97.5% using TCFA(4 g/L). It was

**Table 4** Effect of modification process on CFA adsorption capacity

Initial dye concentration (mg/L)	Treated coal fly ash		
	Optimum TCFA dose (g/L)	Loading (mg/g)	Removal %
10	2	4.99	99.7
20	3	6.49	97.4
30	4	7.32	97.5

reported in the literature that high loadings of raw coal fly ash are required for dyes removal (Eteba et al.2021).

Effect of adsorption time on dye elimination

Figure 9a and b shows the effect of adsorption time on both dye removal (%) and maximum loading of TCFA adsorbent. It was noticed that the percentage of dye removal increased as contact time increases within 30 min. The optimum removal efficiency (equilibrium concentration C_e) was

Fig. 9 **a** Effect of adsorption time on dye elimination (temperature 20 °C, pH (8.60), mixing speed 500 r.p.m, adsorbent dose 1 g/L and particles size < 75 μm). **b** Effect of contact time on adsorbent capacity (temperature 20 °C, pH (8.60), mixing speed 500 r.p.m, adsorbent dose 1 g/L and particles size < 75 μm)
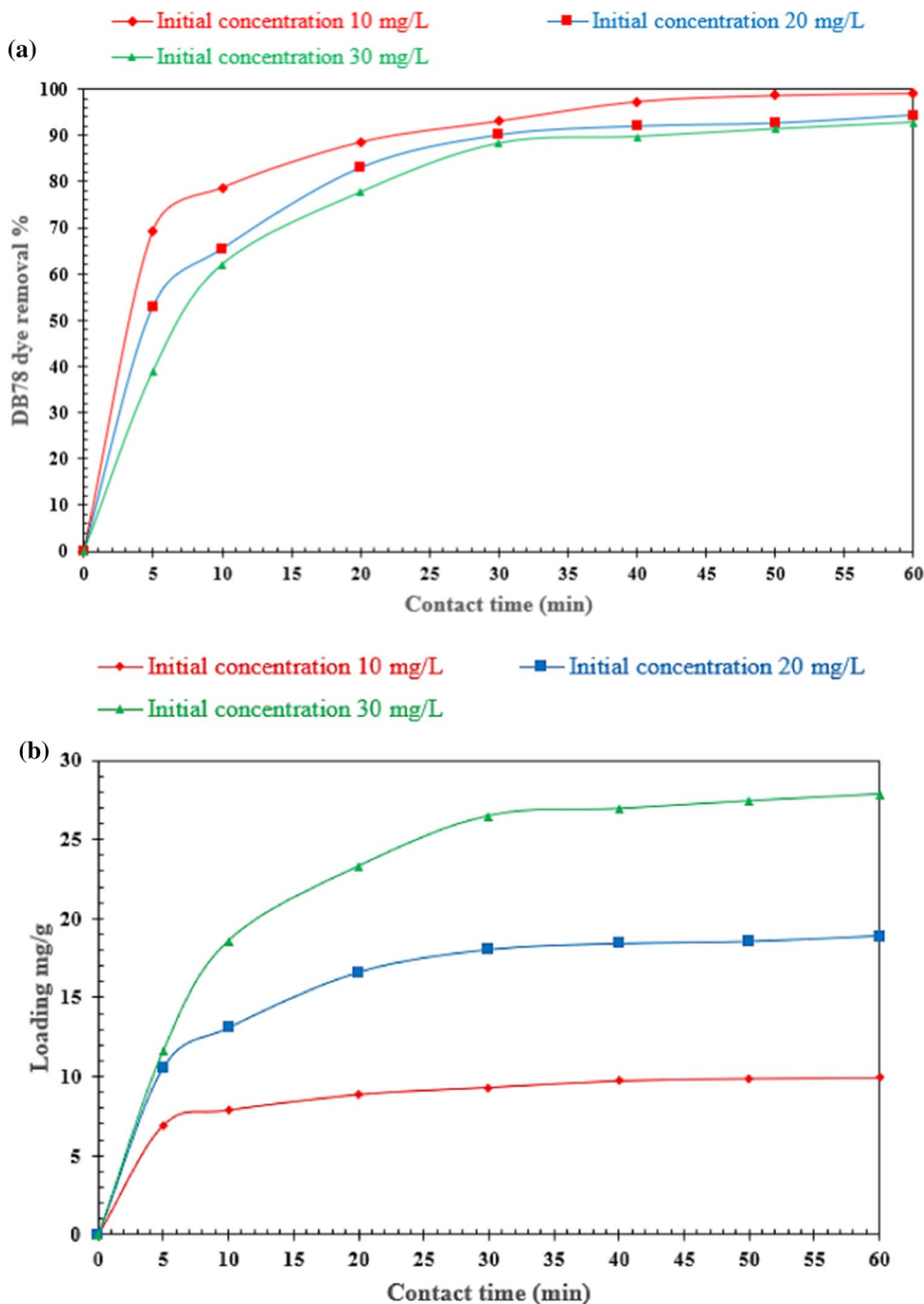
reached at maximum loading capacity (equilibrium loading q_e). It was found that the contact time needed to remove 93.1% of anionic dye at low TCFA dose (1 g/L) and initial dye concentration 10 mg/L is 30 min.

The equilibrium concentration decreased to 1.98 mg/L with dye removal 90.1% and optimum loading capacity 18 mg/g for initial dye concentration 20 mg/l. The equilibrium concentration decreased to 3.52 mg/L with dye removal efficiency 88.3% and optimum loading capacity 26.48 mg/g for initial dye concentration 30 mg/L solution. It was reported that the equilibrium contact time for dye removal using raw coal fly ash is 60 min (Eteba et al. 2021). In the current study, chemical modification using HCl solution decreased the equilibrium time to 30 min. This significant decrease in equilibrium time is attributed to the increase in interaction forces between anionic dyes molecules and H$^+$

ions accumulated on TCFA surface after chemical modification process. Furthermore, the major improvement in CFA surface area increases the number of adsorption active sites on particles surface. This increasing of active sites on CFA surface leads to increase in the adsorption capacity of TCFA and decreases in the equilibrium contact time.

Effect of initial concentration of DB78 on adsorption

The removal (%) of direct blue 78 (DB78) dye solutions was studied using initial concentrations of 10, 20 and 30 mg/L. Figure 10a shows that removal % decreased from 99.7 to 88.3% when initial concentration of DB78 increased from 10 to 30 mg/L at TCFA dose 1 g/L. Similar behavior was observed using TCFA dose 2 g/L and 3 g/L. Notably, the initial concentration of DB showed no influence on DB78

Fig. 10 a Effect of primary concentration on direct blue 78 dye removal (temperature 20 °C, pH (8.6), mixing speed 500 r.p.m, contact time 30 min and particles size < 75 μm). b Effect of initial concentration on adsorbent capacity (temperature 20 °C, pH (8.60), mixing speed 500 r.p.m, contact time 30 min and particles size < 75 μm)
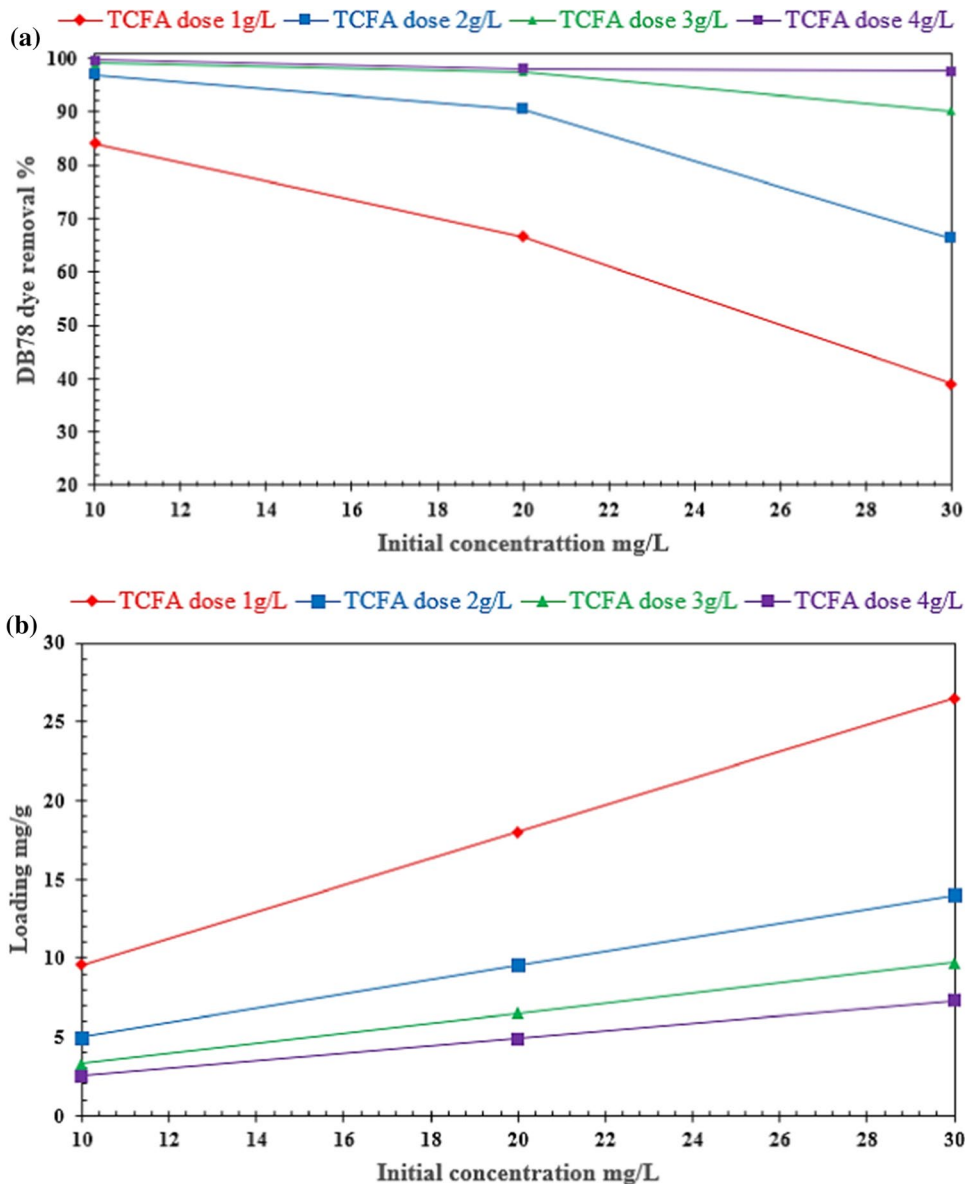
removal % when TCFA dose is 4 g/L. This is due to the presence of free adsorption sites on TCFA particles that are able to attach higher number of DB 78 molecules. Figure 10b shows that the adsorption capacity increases with increasing initial dye concentration at constant adsorbent dose and contact time. The adsorbent capacity increased from 9.5 to 26.5 mg/g as initial dye concentration increased from 10 to 30 mg/L using TCAF 1 g/L. The adsorbent capacity increased from 3.3 to 9.7 mg/L when the initial concentration of the dye added from 10 to 30 mg/L using TCAF 4 g/L.

Adsorption isotherm

The adsorption isothermal shown in Fig. 11 shows the quantity of adsorbate (DB78) dye that would be adsorbed by TCFA (q_e) against the dye concentration in the liquid phase (C_e). These findings are necessary to design adsorption system. Also, the form of the equilibrium curve helps describe other phenomena linked with the adsorbent–adsorbate interaction (Sun et al. 2013). The equilibrium curves are identified in four main classes according to the primary slope and subgroups are described for each class, based on upper parts shapes and slope changes. (a) S curves or vertical orientation isotherm, (b) L curves, normal or "Langmuir" isotherms, (c) H curves or high-affinity isotherms or (d) C curves or constant partition isotherm (Dizge et al. 2008). The findings in Fig. 11 showed that the adsorption takes places within relatively weak forces such as van der Waals forces. L shape well-presented the adsorption isotherm.

Higher adsorption capacity is found as adsorbate concentrations increase when the adsorption available sites numbers are limited. According to the availability of accessible adsorption sites on the surface of adsorbent, a competition between adsorptive molecules would occur in order to reach these sites. Several isothermal models were developed to present the adsorption relationship. As has been previously reported in the literature, the Freundlich and Langmuir isotherms are the most employed models for interpretation of the adsorption process (Yuan et al. 2019).

The Freundlich isotherm believes that the adsorption takes place on a heterogeneous surface, and the adsorbed mass increases exponentially with an increase in concentration (Chiou et al. 2004). This isotherm explains equilibrium on heterogeneous surfaces and hence capacity is not presumed monolayer. In liquid phase, this isotherm is given by Eq. (1):

$$Q_e = K_f C_f^{1/n} \tag{1}$$

where k_F is the Freundlich fixed value (K_F unit = mg/g where $c = 1/n_f$ is the heterogeneity factor). This isotherm focuses on integrating the function of adsorbent–adsorbate surface interactions. Figure 12 indicates the application of equilibrium data according to Freundlich isotherm. The Freundlich constant k_f values are 7.48, 7.04 and 6.57 and the heterogeneity factor $1/n_f$ values are 0.353, 0.523 and 0.616 for dye solution with initial concentration 10, 20 and 30 mg/L, respectively. The higher ($1/n_f$), the less the adsorbate can be adsorbed. Thus, $n_f < 1$ is preferable for Freundlich isotherm model.

The Langmuir isotherm believes that sorption occurs within the adsorbent at different homogeneous sites and was effectively applied to several processes of adsorption. The isotherm's physical simplicity is based on some assumptions

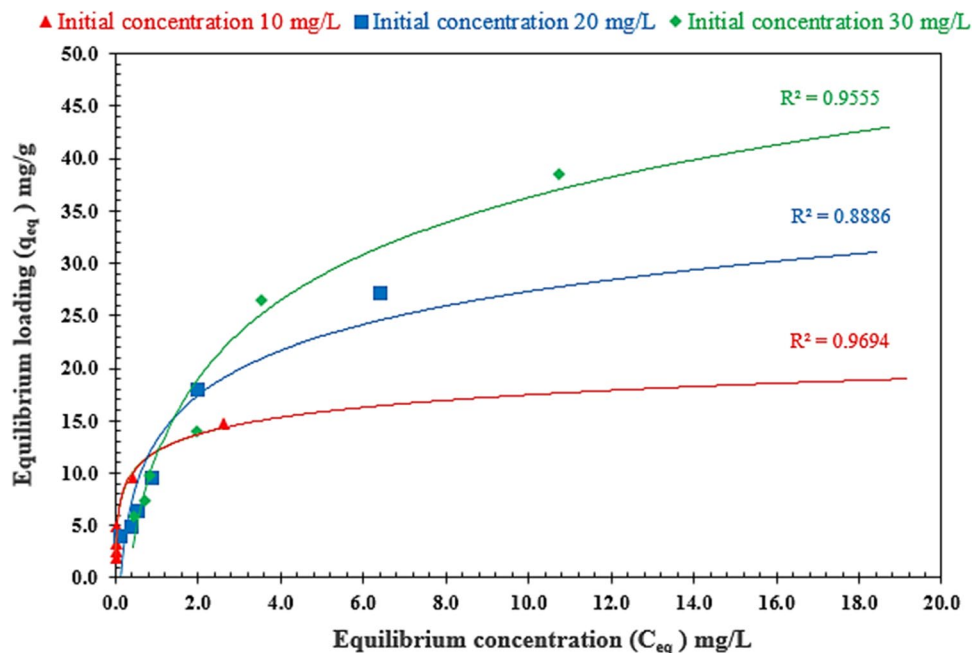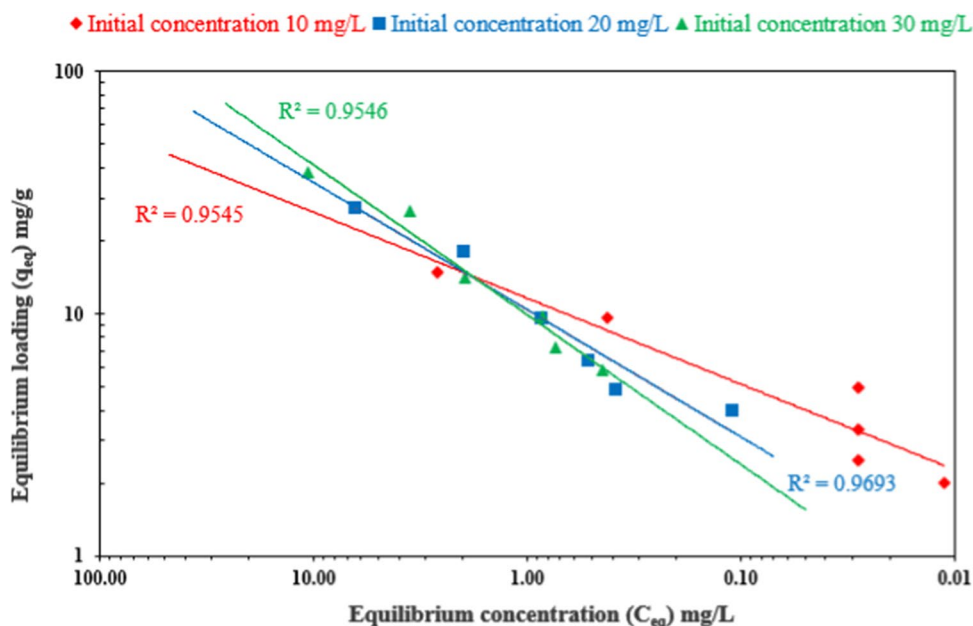**Fig. 11** Adsorption isotherm of TCFA for direct blue 78 dye removal

Fig.12 Freundlich adsorption isotherm of TCFA for direct blue 78 dye

(Yuan et al. 2019): Adsorption cannot happen elsewhere monolayer. Each site can get one solute molecule only. The adsorbent surface is uniform and all of its sites are energetically equipollent. The linear form of Langmuir isotherm is given by the following equation Eq. (2):

$$(C_e/qe) = (1/Q_0 b) + (C_e/Q_0) \qquad (2)$$

where C_e is the equilibrium concentration (mg/L), q_e the mass adsorbed at equilibrium (mg/g), Q_0 the adsorbent loading (mg/g) and b is the adsorption energy (Langmuir fixed value L/mg). The values of Q_0 and b were determined from the slope and intercept of the linear plots C_e/q_e versus C_e, resulting in a straight line of slope $1/Q_0$ corresponding to the total coverage of monolayer (mg/g) and the intercept is $1/Q_0 b$ (Dizge et al. 2008). Figure 13 indicates the application of equilibrium data according to Langmuir isotherm. The adsorbent loading values (Q_0) are 15.29 mg/g, 34.96 mg/g and 53.76 mg/g Langmuir fixed value (b) values are 8.175 L/mg, 0.521 L/mg and 0.235 L/mg for solution with initial concentration 10, 20 and 30 mg/L, respectively.

Adsorption isothermal models are summarized in Table 5, followed closely Freundlich and Langmuir isotherm, respectively. The latter isotherm is better suited to the results of

Fig. 13 Langmuir adsorption isotherm of TCFA for direct blue 78 dye removal
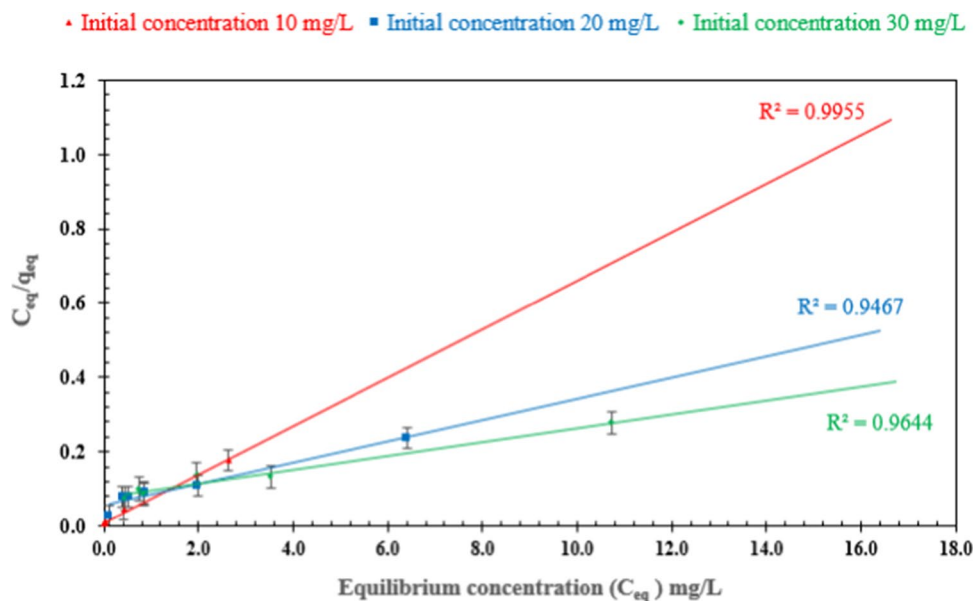
Table 5 Comparison of adsorption isothermal models

Initial concentration (mg/L)	Direct blue 78 dye adsorption					
	Langmuir isothermal			Freundlich isothermal		
	Q_0 (mg/g)	B (1/mg)	R^2	K_f (mg/g)	nf	R^2
10	15.29	8.175	0.9955	11.58	0.3534	0.9011
20	34.96	0.521	0.9467	10.38	0.5239	0.9455
30	53.76	0.2354	0.9644	9.89	0.6168	0.9711

TCFA-DB75 adsorption system. Similar results were reported by (Hamdaoui et al. 2007; Ghazi Mokri et al. 2015).

Conclusion

The adsorption behavior of treated coal fly ash (TCFA) was experimentally investigated. TCFA was found as an efficient low-cost adsorbent for direct blue 78 (DB78) removal. Thermochemical modification process using HCl solution at 90 °C showed significant improvement in the surface area and adsorption capacity of TCFA. It increased its surface area from 9.6 to 60.4 m^2g^{-1} and improved surface roughness. The FTIR analysis showed that there is no significant difference between TCFA spectrum before and after adsorption process referring to physisorption adsorption. Around 99% of dyes removal can be reached (10–30 mg/L) using small TCAF dose (1–4 g/L). Isotherm class (L shape) well-presented TCAF-DB78 adsorption system. Adsorbed DB 78 dye molecules are aligned on TCFA surface in a homogenous and monolayer form based on Langmuir fitting results. The current study showed that removal of DB78 by mesoporous TCFA made from low-cost industry solid waste is a viable option. This cost-effective adsorbent is recommended for use in textile industries to reduce the treatment expenses of their wastewater treatment facility.

Declarations

References

Abdel-Aziz MH, El-Ashtoukhy EZ, Zoromba MS, Bassyouni M, Sedahmed GH (2020) Removal of nitrates from water by electrocoagulation using a cell with horizontally oriented Al serpentine tube anode. J Ind Eng Chem 82:105–112

Al-Ghouti MA, Khraisheh MAM, Allen SJ, Ahmad MN (2003) The removal of dyes from textile wastewater: a study of the physical characteristics and adsorption mechanisms of diatomaceous earth. J Environ Manage 69(3):229–238

Anastopoulos I, Bhatnagar A, Hameed BH, Ok YS, Omirou M (2017) A review on wastederived adsorbents from sugar industry for pollutant removal in water and wastewater. J Mol Liq 240:179–188. https://doi.org/10.1016/j.molliq.2017.05.063

Astuti W, Chafidz A, Wahyuni ET, Prasetya A, Bendiyasa IM, Abasaeed AE (2019) Methyl violet dye removal using coal fly ash (CFA) as a dual sites adsorbent. J Environ Chem Eng 7(5):103262

Bada SO, Potgieter-Vermaak S (2008) Evaluation and treatment of coal fly ash for adsorption application. Leonardo Electron J Pract Technol 12:37–48

Banerjee S, Sharma GC, Chattopadhyaya MC, Sharma YC (2014) Kinetic and equilibrium modeling for the adsorptive removal of methylene blue from aqueous solutions on of activated fly ash (AFSH). J Environ Chem Eng 2(3):1870–1880

Bansal RC, Goyal M (2005) Activated carbon adsorption. CRC Press

Bassyouni M, Mansi AE, Elgabry A, Ibrahim BA, Kassem OA, Alhebeshy R (2020) Utilization of carbon nanotubes in removal of heavy metals from wastewater: a review of the CNTs' potential and current challenges. Appl Phys A 126(1):1–33

Blissett RS, Rowson NA (2012) A review of the multi-component utilisation of coal fly ash. Fuel 97:1–23

Bonilla-Petriciolet A, Mendoza-Castillo DI, Reynel-Ávila HE (eds) (2017) Adsorption processes for water treatment and purification. Springer, Netherlands

Chiou MS, Ho PY, Li HY (2004) Adsorption of anionic dyes in acid solutions using chemically cross-linked chitosan beads. Dyes Pigm 60(1):69–84

Crini G (2006) Non-conventional low-cost adsorbents for dye removal: a review. Biores Technol 97(9):1061–1085

Crini G, Lichtfouse E, Wilson LD, Morin-Crini N (2019) Conventional and non-conventional adsorbents for wastewater treatment. Environ Chem Lett 17(1):195–213

da Costa Rocha AC, Scaratti G, Moura-Nickel CD, da Silva TL, Gurgel Adeodato Vieira M, Peralta RM, Peralta Muniz Moreira RDF (2020) Economical and technological aspects of copper removal from water using a geopolymer and natural zeolite. Water, Air, Soil Pollut 231(7):1–15

Dizge N, Aydiner C, Demirbas E, Kobya M, Kara S (2008) Adsorption of reactive dyes from aqueous solutions by fly ash: kinetic and equilibrium studies. J Hazard Mater 150(3):737–746

Elhenawy Y, Elminshawy NA, Bassyouni M, Alanezi AA, Drioli E (2020) Experimental and theoretical investigation of a new air gap membrane distillation module with a corrugated feed channel. J Membr Sci 594:117461

Eteba A, Bassyouni M, Saleh M (2021) Removal of hazardous organic pollutants using fly ash. Environ Ecol Res 9(4):196–203

Fauzi A, Nuruddin MF, Malkawi AB, Abdullah MMAB (2016) Study of fly ash characterization as a cementitious material. Procedia Eng 148:487–493

Ferrero F (2015) Dye removal from aqueous solution using coal fly ash for continuous flow adsorption. Clean Technol Environ Policy 17(7):1907–1915

Gao M, Ma Q, Lin Q, Chang J, Bao W, Ma H (2015) Combined modification of fly ash with Ca (OH) 2/Na2FeO4 and its adsorption of Methyl orange. Appl Surf Sci 359:323–330

Ghazi Mokri HS, Modirshahla N, Behnajady MA, Vahid B (2015) Adsorption of CI Acid Red 97 dye from aqueous solution onto walnut shell: kinetics, thermodynamics parameters, isotherms. Int J Environ Sci Technol 12(4):1401–1408

Golbad S, Khoshnoud P, Abu-Zahra N (2017) Hydrothermal synthesis of hydroxy sodalite from fly ash for the removal of lead ions from water. Int J Environ Sci Technol 14(1):135–142

Gong R, Zhu S, Zhang D, Chen J, Ni S, Guan R (2008) Adsorption behavior of cationic dyes on citric acid esterifying wheat straw: kinetic and thermodynamic profile. Desalination 230(1–3):220–228

Gutub SA, Bassyouni M, Abdel-Hamid SMS (2013) Dissolved solids adsorption of freshwater using synthesized bio-foam composite. Life Sci J 10(2):464–471

Hamdaoui O, Naffrechoux E (2007) Modeling of adsorption isotherms of phenol and chlorophenols onto granular activated carbon: part I. Two-parameter models and equations allowing determination of thermodynamic parameters. J Hazard Mater 147(1–2):381–394

Hussain Z, Chang N, Sun J, Xiang S, Ayaz T, Zhang H, Wang H (2022) Modification of coal fly ash and its use as low-cost adsorbent for the removal of directive, acid and reactive dyes. J Hazard Mater 422:126778

Jeyageetha CJ, Kumar SP (2016) Study of SEM/EDXS and FTIR for fly ash to determine the chemical changes of ash in marine environment. Int J Sci Res 5:1688–1692

Lellis B, Fávaro-Polonio CZ, Pamphile JA, Polonio JC (2019) Effects of textile dyes on health and the environment and bioremediation potential of living organisms. Biotechnol Res Innov 3(2):275–290

Mor S, Chhavi MK, Sushil KK, Ravindra K (2018) Assessment of hydrothermally modified fly ash for the treatment of methylene blue dye in the textile industry wastewater. Environ Dev Sustain 20(2):625–639

Mushtaq F, Zahid M, Mansha A, Bhatti IA, Mustafa G, Nasir S, Yaseen M (2020) MnFe2O4/coal fly ash nanocomposite: a novel sunlight-active magnetic photocatalyst for dye degradation. Int J Environ Sci Technol 17(10):4233–4248

Qi Y, Yang M, Xu W, He S, Men Y (2017) Natural polysaccharides-modified graphene oxide for adsorption of organic dyes from aqueous solutions. J Colloid Interface Sci 486:84–96

Rubab M, Bhatti IA, Nadeem N, Shah SAR, Yaseen M, Naz MY, Zahid M (2021) Synthesis and photocatalytic degradation of rhodamine B using ternary zeolite/WO3/Fe3O4 composite. Nanotechnology 32(34):345705

Sarkar A, Saha M, Saha JK, Vassanda Coumar M, Mandal A, Patra AK (2022) Comparative assessment of P adsorption, release kinetics, enzymatic activities of weathered fly ash amended texturally different soils. Int J Environ Sci Technol 19(3):2089–2106

Scalbi S, Tarantini M, Mattioli D (2005) Efficient use of water in the textile finishing industry.

Siyal AA, Shamsuddin R, Low A, Hidayat A (2020) Adsorption kinetics, isotherms, and thermodynamics of removal of anionic surfactant from aqueous solution using fly ash. Water Air Soil Pollut 231(10):1–13

Sun D, Zhang X, Wu Y, Liu T (2013) Kinetic mechanism of competitive adsorption of disperse dye and anionic dye on fly ash. Int J Environ Sci Technol 10(4):799–808

Wang X, Jiang C, Hou B, Wang Y, Hao C, Wu J (2018) Carbon composite lignin-based adsorbents for the adsorption of dyes. Chemosphere 206:587–596

Yuan N, Cai H, Liu T, Huang Q, Zhang X (2019) Adsorptive removal of methylene blue from aqueous solution using coal fly ash-derived mesoporous silica material. Adsorpt Sci Technol 37(3–4):333–348

Zarrini K, Rahimi AA, Alihosseini F, Fashandi H (2017) Highly efficient dye adsorbent based on polyaniline-coated nylon-6 nanofibers. J Clean Prod 142:3645–3654